Screening effect in spin Hall devices

M. Creff and J.-E. Wegrowe *
LSI, École Polytechnique, CEA/DRF/IRAMIS, CNRS, Institut Polytechnique de Paris, 91120 Palaiseau, France

E. Olive
GREMAN UMR-CNRS 7347, Universit de Tours, INSA Centre Val de Loire, Parc de Grandmont, 37200 Tours, France

(Received 21 December 2021; revised 11 March 2022; accepted 29 April 2022; published 16 May 2022)

The stationary state of the spin Hall bar is studied in the framework of a variational approach that includes nonequilibrium screening effects at the edges. The minimization of the power dissipated in the system is performed taking into account the spin-flip relaxation and the global constraints due to the electric generator and global charge conservation. The calculation is performed within the approximations of negligible spin-flip scattering and strong spin-flip scattering. In both cases, simple expressions of the spin accumulation and the longitudinal and transverse pure spin currents are derived analytically. In usual conditions, the maximum amplitude of the spin accumulation is expected to be of the order of 1% of the equilibrium density carriers.

DOI: 10.1103/PhysRevB.105.174419

I. INTRODUCTION

Spin accumulation can be produced at the edges of a conducting bar at zero external magnetic field by injecting an electric current into a nonmagnetic material with high spin-orbit coupling [1–9]. This effect is called spin Hall effect (SHE). It has been predicted some decades ago [10] and described in the framework of various theoretical models [11–19]. However, a description that takes into account the *nonequilibrium nature of the electric screening* occurring in the SHE is still an open problem. One of the main difficulties is the same as for the classical Hall effect [20–29]; it is due to the fact that the values of the charge and spin accumulation at the edges of the Hall bar are not directly imposed by the external constraints. Instead, for the stationary state, the accumulation of electric charges and spins at the edges is generated by the system itself, in reaction to the action of the magnetic field (the spin-orbit effective magnetic field in the case of SHE), together with stationary current injected from the electric generator. As a consequence, the determination of a unique solution to the spin-dependent drift-diffusion equations at stationary state—which necessitates *local boundary conditions*—is problematic [14].

It is, however, possible to take into account the nonequilibrium nature of the electric screening in the case of a ideal Hall bar [30–35] on the basis of the least dissipation principle [36–38]. The global constraints applied to the system (current injection, global charge conservation, and geometry) are used instead of the local boundary conditions. The usual physical picture of the Hall effect without spin is then slightly modified. Indeed, it can be shown [33] that the charges accumulated at the edges of the usual Hall bar are not static but generate a *nonuniform longitudinal current* $\delta J_x(y)$. Physically, this surface current is responsible for the well-known robustness of the Hall voltage, which can be measured while using a good or a bad voltmeter (i.e., with huge variations of the electric leakage at the edges [39]), because the electric charges accumulated are renewed permanently despite the zero transverse current. Furthermore, if a secondary passive circuit is contacted at the two edges of the Hall bar, the variational method shows that the electric current injected is mainly carried by the longitudinal surface currents $\delta J_x(y)$ instead of the transverse current J_y [35].

The question then arises about the application of this variational approach to the SHE in a spin Hall bar. Is the physical picture modified? Is it possible to calculate the amplitude of the spin accumulation and that of the pure spin currents without assuming arbitrary values for the boundary conditions at the edges? The goal of the present work is to answer to these questions. The analysis is based on the two spin channel model, which has been intensively used in the context of giant magnetoresistance [40–45], spin-injection [46–48], and SHE [12–15,17,49].

The paper is organized in six sections. In Sec. II below, we introduce the system under study and the formalism used for the model. For the sake of clarity the derivation of the spin accumulation and currents is first performed in the case of negligible spin-flip scattering in Sec. III. The Joule functional is minimized under the global constraints, and the stationarity condition for the electric current $\vec{J}$ is obtained. The spin accumulation is then derived by integration of the Maxwell-Gauss equation. In Sec. IV, the same derivation for the currents and the spin accumulation is performed taking into account the spin-flip dissipation under the assumption of strong spin-flip scattering. It is shown that the spin-flip scattering imposes a transverse pure spin current, and the profile of the spin accumulation is now composed of a linear part and an exponential part. In Sec. V, the expressions for the spin accumulation and the charge accumulation are discussed from a quantitative viewpoint. Surprisingly, the quantitative analysis seems to show that the exponential part of the spin

*jean-eric.wegrowe@polytechnique.edu

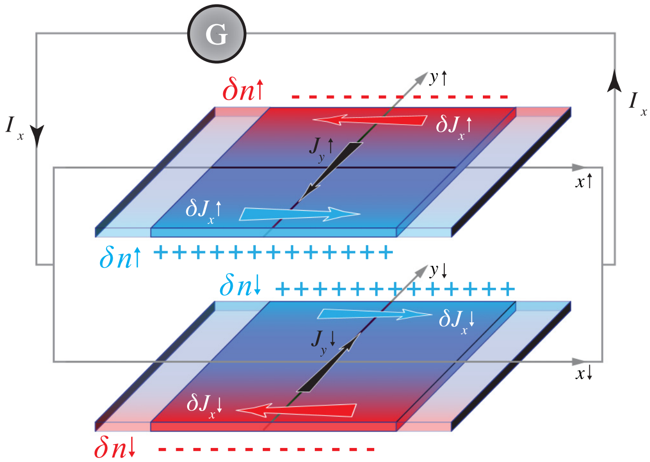

FIG. 1. Schematic representation of the two channel model (corresponding to spin ↑ and spin ↓) for a spin Hall bar. The device is contacted to an electric generator that imposes a longitudinal stationary current J_x^0 (not shown). The charge accumulations $\pm\delta n_\updownarrow$ and the inhomogeneous part of the longitudinal currents $\delta J_{x\updownarrow}(y) = J_{x\updownarrow}(y) - J_x^0$ are represented at both edges for each channel together with the transverse current $J_{y\updownarrow}$ flowing from one edge to the other.

accumulation is negligible with respect to the linear part in usual conditions. The main results are summarized in the conclusion (Sec. VI).

II. THE MODEL

Before introducing the formalism, we first present an intuitive physical picture of the system under study as sketched in Figs. 1 and 2. As pointed out in the Introduction, the model is based on the two-channel approximation, which is a convenient description that assumes the separation of the typical timescales between the slow spin-flip relaxation rate (internal variable described by the index $\updownarrow$ below) and the fast spin-conserved electronic relaxation rates. In other terms, the two spin channels ↑ and ↓ are well defined because the interchannel relaxation time is much larger than the intrachannel relaxation times. In particular, the electric charges relax toward the local equilibrium state inside each spin channel before spin-flip relaxation occurs. As a consequence, the nonzero stationary charge-accumulation $\delta n_\updownarrow \neq 0$ is generated separately inside each spin channel, even if the total density of the electric charges at the surface is homogeneous.

Without spin-flip scattering, the spin Hall bar is then equivalent to a superimposition of two classical Hall bars submitted to an effective spin-orbit magnetic field acting in opposite directions but equal amplitudes (see Figs. 1 and 2). The typical behavior due to the screening observed in the usual Hall bar [33–35] could then be extrapolated also for the spin Hall bar (with the presence of longitudinal pure spin current near the edges). However, the coupling between the two channels due to both the electrostatic interaction [see Eq. (2) below] and the spin-flip scattering renders the problem less intuitive. The minimization of the dissipation functional is then necessary in order to obtain analytical expressions. This is the reason why we apply the variational method to the SHE with neglecting the spin-flip scattering in a first step (the next section), and we study the effects due to the addition of a strong spin-flip scattering in a second step (Sec. IV).

The system is a long bar of width 2ℓ and thickness d composed of a thin layer of a nonmagnetic material with strong spin-orbit coupling contacted to an electric generator. We assume that the bar is invariant by translation along its longitudinal axis x (i.e., we do not take into account the region close to the generator nor the perturbation caused by possible lateral contacts), that the lateral edges are symmetric, that the device is planar (no charge transport in the z direction) and that the polarization axis of the spins is oriented along the z direction. In the framework of the two-channel model, the charge carriers are separated into two populations that are the charge carriers of spin up ↑ and the charge carriers of spin down ↓ with the respective charge-densities $n_\uparrow$ and $n_\downarrow$.

The conductor is characterized by a density of charge-carriers $n^Q \equiv n_\uparrow + n_\downarrow = 2n_0 + \delta n^Q$, where $2n_0$ is the density defined by electroneutrality at equilibrium (i.e., without current injected). Accordingly, n_0 is uniform and does not depend on the spin channel. On the other hand, $\delta n^Q(y)$ is the charge accumulation, which is not a function of x due to the invariance by translation and is the sum of the charge accumulation for each spin channel: $\delta n^Q(y) = \delta n_\uparrow(y) + \delta n_\downarrow(y)$. The Coulomb interaction is described by the electric potential V that follows the Poisson law $\nabla^2 V = -q\delta n^Q/\epsilon$, where q is the charge of the carriers, ϵ is the permittivity of the material, and $\vec{\nabla} = \{\partial_x, \partial_y\}$ is the gradient operator in 2D.

The energy of the system is then defined by the two chemical potentials $\mu_\uparrow$ and $\mu_\downarrow$ such that

$$\mu_\updownarrow = \frac{kT}{q} \ln\left(\frac{n_\updownarrow}{n_0}\right) + V + \mu_\updownarrow^{ch}, \tag{1}$$

where k is the Boltzmann constant, T is equal to the temperature of the material in the case of nondegenerate semiconductors, or T is equal to the Fermi temperature $T \equiv T_F$ in the case of degenerate semiconductors and metals [50]. The first term on the right-hand side accounts for the diffusion of the carriers (this term is justified in the framework of the

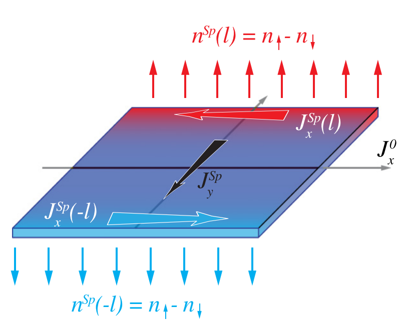

FIG. 2. Superimposition of the two channels represented for the symmetric device and environment ($C_E = 0$ in the text). The electric generator and the injected current J_x^0 are not shown for clarity. The system is characterized by the absence of the total charge accumulation, the spin accumulation $n^{Sp}(y) = \delta n_\uparrow(y) - \delta n_\downarrow(y)$ with opposite directions at the two edges, the inhomogeneous part of the longitudinal spin currents $J_x^{Sp}(y) = J_{x\uparrow}(y) - J_{x\downarrow}(y)$, and the transverse spin current $J_y^{Sp} = J_{y\uparrow}(y) - J_{y\downarrow}(y)$.

local equilibrium approximation [49,51]). The second term describes the electric potential V. The third term $\mu^{ch}_{\updownarrow}$ is the pure chemical potential that accounts for the spin-flip scattering and is the main parameter for the description of giant magnetoresistance effects [40–42,44–46]. In the following, we assume that $\mu^{ch}_{\updownarrow}$ is uniform in order to treat uniquely the spin accumulation due to the SHE in a homogeneous Hall bar. The electric field reads $\vec{\mathcal{E}} = -\vec{\nabla} V = \mathcal{E}^0_x\,\vec{e}_x + \mathcal{E}_y\,\vec{e}_y$, where the x-component $\mathcal{E}^0_x$ is constant (due to the invariance along x), so that the Poisson law is reduced to $\partial_y \mathcal{E}_y = q\delta n^Q/\epsilon$. Note that the electric field does not depend on the spin channel, so that the electric potential V couples the two channels in Eq. (1). We can rewrite the Poisson law with the help of the chemical potential Eq. (1) as follows:

$$\nabla^2 \mu_{\updownarrow} - \lambda_D^2 \frac{q n_0}{\epsilon} \nabla^2 \ln\left(\frac{n_{\updownarrow}}{n_0}\right) + \frac{q\delta n^Q}{\epsilon} = 0, \tag{2}$$

where $\lambda_D = \sqrt{\frac{kT\epsilon}{q^2 n_0}}$ is the well-known Debye-Fermi screening length.

On the other hand, the transport equations for the charge carriers are given by the Ohm's law for each channel,

$$\vec{J}_{\updownarrow} = -\hat{\sigma}_{\updownarrow}\,\vec{\nabla}\mu_{\updownarrow} = -q n_{\updownarrow}\hat{\eta}_{\updownarrow}\,\vec{\nabla}\mu_{\updownarrow}, \tag{3}$$

where $\hat{\sigma}_{\updownarrow} \equiv q n_{\updownarrow}\hat{\eta}_{\updownarrow}$ is the spin-dependent conductivity tensor, and $\eta_{\updownarrow}$ is by definition the electric mobility tensor. As a consequence of both the Onsager reciprocity relations [52] and the property of the spin-orbit effective fields, the mobility tensor takes the following form in the orthonormal basis $\{\vec{e}_{x_\uparrow}, \vec{e}_{y_\uparrow}, \vec{e}_{x_\downarrow}, \vec{e}_{y_\downarrow}\}$ (see Fig. 1):

$$\hat{\eta}_{\updownarrow} = \eta \begin{pmatrix} 1 & \theta_{\rm so} & 0 & 0 \\ -\theta_{\rm so} & 1 & 0 & 0 \\ 0 & 0 & 1 & -\theta_{\rm so} \\ 0 & 0 & \theta_{\rm so} & 1 \end{pmatrix},$$

where η is the mobility of the material and $\theta_{\rm so}$ is the spin Hall angle. The two diagonal submatrices are not coupled; this is due to the fact that the two spin channels are well defined, as discussed above. Note that the description holds whatever the underlaying microscopic spin Hall mechanism (intrinsic, extrinsic, orbital, etc.), as long as an internal effective magnetic field can be defined. In usual conditions, the amplitude of the spin Hall mobility $\eta\theta_{\rm so}$ is proportional to the amplitude of the effective magnetic field. The transport equation reads

$$\vec{J}_{\updownarrow} = -q n_{\updownarrow}\eta(\vec{\nabla}\mu_{\updownarrow} \mp \theta_{\rm so}\,\vec{e}_z \times \vec{\nabla}\mu_{\updownarrow}), \tag{4}$$

where the symbols $\mp$ refer to spin channel $\uparrow$ for the upper sign and spin channel $\downarrow$ for the lower sign. This equation is equivalent to the Dyakonov-Perel equation of the SHE if one considers only the projection of the spins over the perpendicular axis [49]. It is convenient to rewrite Eq. (4) in the following forms:

$$-q n_{\updownarrow}\eta\left(1+\theta_{\rm so}^2\right)\partial_x \mu_{\updownarrow} = J_{x\updownarrow} \mp \theta_{\rm so} J_{y\updownarrow} \tag{5}$$

$$-q n_{\updownarrow}\eta\left(1+\theta_{\rm so}^2\right)\partial_y \mu_{\updownarrow} = J_{y\updownarrow} \pm \theta_{\rm so} J_{x\updownarrow} \tag{6}$$

$$\|\vec{J}_{\updownarrow}\|^2 \equiv J^2_{x\updownarrow} + J^2_{y\updownarrow} = (q n_{\updownarrow}\eta)^2\left(1+\theta_{\rm so}^2\right)\|\vec{\nabla}\mu_{\updownarrow}\|^2. \tag{7}$$

The power dissipated by the charge carriers in each spin channel is the Joule power,

$$P_{J\updownarrow} = S_{\rm lat}\int_{-\ell}^{\ell} q n_{\updownarrow}\eta\|\vec{\nabla}\mu_{\updownarrow}\|^2 dy = \frac{S_{\rm lat}}{q n_0\eta\left(1+\theta_{\rm so}^2\right)}\int_{-\ell}^{\ell}\frac{n_0}{n_{\updownarrow}}\|\vec{J}_{\updownarrow}\|^2 dy,$$

where we have introduced the lateral surface $S_{\rm lat} = L_x\,d$, where L_x is the length of the Hall bar along the x direction.

On the other hand, the power dissipated by the spin-flip scattering (i.e., the transition of an electric charge from one spin channel to the other) per unit of volume reads $\mathcal{L}\,\Delta\mu^2$, where $\Delta\mu = \mu_\uparrow - \mu_\downarrow$ and $\mathcal{L}$ is the Onsager transport coefficient describing the spin-flip relaxation rate in the framework of the two-channel model [31,41,42,44,49]. The coefficient $\mathcal{L}$ is a property of the material which is related to the measured *spin-flip scattering length* $l_{\rm sf}$ by the relation [49]

$$\mathcal{L} = \frac{\sigma_0}{2 l_{\rm sf}^2}, \tag{8}$$

where σ_0 is the conductivity. In the framework of the variational approach, and ignoring temperature gradient, the stationary state is defined by the principle of *least power dissipation* [37,38]. In other terms, the distribution of charge densities and currents is determined by the state of minimum power production, taking into account the global constraints applied to the system. These constraints are due to the presence of the electric generator, the electrostatic boundary conditions, and the symmetries of the device [30,31,33–35]. Due to the *electroneutrality* and the fact that the device is symmetric, the integral of the total charge accumulated in the two channels cancels out $\int_{-\ell}^{\ell}(\delta n_\uparrow + \delta n_\downarrow)dy = 0$, or, in other terms,

$$\frac{1}{2\ell}\int_{-\ell}^{\ell}(n_\uparrow(y) + n_\downarrow(y))dy = 2n_0. \tag{9}$$

On the other hand, the generator injects a constant current through the device, so that the integrated current density is constant,

$$\frac{1}{2\ell}\int_{-\ell}^{\ell}(J_{x\uparrow}(y) + J_{x\downarrow}(y))dy = 2J_x^0. \tag{10}$$

III. SHE WITH NEGLIGIBLE SPIN-FLIP SCATTERING

The approximation of negligible spin-flip scattering corresponds to the case $l_{\rm sf} \gg \ell$ where ℓ is the width of the spin Hall bar. Let use define the reduced power, $\tilde{P}_{J\updownarrow} = \frac{q\eta(1+\theta_{\rm so}^2)}{S_{\rm lat}} P_{J\updownarrow} = \int_{-\ell}^{\ell}\frac{J^2_{x\updownarrow}+J^2_{y\updownarrow}}{n_{\updownarrow}}dy$. We shall use the Lagrange multipliers λ_J and λ_n in order to take into account the constraints, respectively, Eq. (9) and Eq. (10) in the minimization of the functional $\mathcal{F}$,

$$\mathcal{F}_{J\updownarrow}[J_{x\updownarrow}, J_{y\updownarrow}, n_{\updownarrow}] = \int_{-\ell}^{\ell}\left(\frac{J^2_{x\updownarrow}+J^2_{y\updownarrow}}{n_{\updownarrow}} - \lambda_J\,(J_{x\uparrow}+J_{x\downarrow}) - \lambda_n\,(n_\uparrow + n_\downarrow)\right)dy. \tag{11}$$

The minimum of the reduced Joule power $\mathcal{F}_J = \tilde{\mathcal{P}}_{J\uparrow} + \tilde{\mathcal{P}}_{J\downarrow}$ corresponds to

$$\frac{\boldsymbol{\delta}\mathcal{F}_{J\updownarrow}}{\boldsymbol{\delta}J_{x\updownarrow}} = 0 \iff 2J_{x\updownarrow} = n_\updownarrow \lambda_J, \tag{12}$$

$$\frac{\boldsymbol{\delta}\mathcal{F}_{J\updownarrow}}{\boldsymbol{\delta}J_{y\updownarrow}} = 0 \iff J_{y\updownarrow} = 0, \tag{13}$$

$$\frac{\boldsymbol{\delta}\mathcal{F}_{J\updownarrow}}{\boldsymbol{\delta}(n_\updownarrow)} = 0 \iff J_{x\updownarrow}^2 + J_{y\updownarrow}^2 = -\lambda_n n_\updownarrow^2. \tag{14}$$

Using Eqs.(9), Eqs.(10), and Eq. (12) leads to $\lambda_J = \frac{2J_x^0}{n_0}$ so that $J_{x\updownarrow} = \frac{n_\updownarrow}{n_0} J_x^0$. The stationarity conditions for the currents are then defined by the two relations

$$J_{x\updownarrow}(y) = J_x^0 \frac{n_\updownarrow(y)}{n_0} \quad \text{and} \quad J_{y\updownarrow} = 0. \tag{15}$$

Similar to the usual Hall effect, *there is no transverse current* in the device for $\l_{sf} \gg \ell$. The explicit expression of $J_{x\updownarrow}(y)$ is obtained if we know the expression of the densities $n_\updownarrow(y)$; this is the aim of the following paragraph.

Inserting the stationarity conditions Eq. (15) into Eq. (5) and Eq. (6), we deduce $\partial_x \mu_\updownarrow = \partial_x \mu = \frac{-J_x^0}{q n_0 \eta (1+\theta_{so}^2)}$ and $\partial_y \mu_\updownarrow = \mp \frac{\theta_{so} J_x^0}{q n_0 \eta (1+\theta_{so}^2)}$. These two terms are constant so that $\nabla^2 \mu_\updownarrow = 0$ and the chemical potentials $\mu_\updownarrow$ are harmonic functions. Equation (2) reduces to

$$\lambda_D^2 \partial_y^2 \ln\left(1 + \frac{\delta n_\updownarrow}{n_0}\right) = \frac{\delta n^Q}{n_0}. \tag{16}$$

In order to evaluate the global boundary conditions for the electric field, we have to integrate the Maxwell equation $\vec{\nabla} \cdot \vec{\mathcal{E}} = \partial_y \mathcal{E}_y = \frac{q}{\varepsilon} \delta n^Q$ at a given point y_0 inside the material

$$\mathcal{E}_y(y_0) = -\partial_y V(y_0) = \frac{E^\infty}{2} - \frac{q}{2\varepsilon} \int_{-\ell}^{\ell} \delta n^Q(y) \mathrm{sgn}(y - y_0) dy, \tag{17}$$

where E^∞ accounts for possible electric charges in the environment of the spin Hall bar (this is the case if a conducting or insulating layer is deposited on one side of the spin Hall bar). Inserting the chemical potential Eq. (1), the transport equation Eq. (6), and the stationary conditions Eq. (15) yields

$$\pm \lambda_{SH}^0 + \lambda_D^2 \partial_y \ln\left(\frac{n_\updownarrow}{n_0}\right)(y_0) - \frac{C_E}{2} + \frac{1}{2n_0} \int_{-\ell}^{\ell} \delta n^Q(y) \mathrm{sgn}(y - y_0) dy = 0, \tag{18}$$

where the asymmetry of the electric environment is described by the characteristic length $C_E = \frac{\varepsilon E^\infty}{q n_0}$. We have also introduced *the spin Hall characteristic length* proportional to the injected current,

$$\lambda_{SH}^0 = \frac{\varepsilon}{q^2 n_0^2 \eta} \frac{\theta_{so}}{1 + \theta_{so}^2} J_x^0 = \frac{\lambda_D^2}{kT} \left(\frac{\theta_{so}}{1 + \theta_{so}^2}\right) \frac{J_x^0}{n_0 \eta}. \tag{19}$$

The three typical length scales λ_{SH}, λ_D, and C_E in Eq. (18) characterize the system. However, the difference of both spin channels in Eq. (18) gives a simple expression of the spin accumulation $n^{Sp} = \delta n_\uparrow - \delta n_\downarrow$ across the spin Hall bar; at the first order in $\delta n_\updownarrow / n_0$, this is a line with a slope defined by the ratio $\lambda_{SH}^0 / \lambda_D^2$ only. We have

$$\frac{n^{Sp}(y)}{n_0} = -2 \frac{\lambda_{SH}^0}{\lambda_D^2} y = -2 \left(\frac{\theta_{so}}{1 + \theta_{so}^2}\right) \left(\frac{q \Delta V}{kT}\right) \frac{y}{L}, \tag{20}$$

where we have introduced the longitudinal voltage ΔV on the right-hand side in order to compare the energy imposed by the generator $q \Delta V$ with the thermal energy kT, as illustrated in Fig. 3(b). The voltage ΔV is measured along the axis x over the distance L and is given by the relation $\Delta V = \mathcal{E}_x^0 L = L J_x^0 / \sigma_0$. Note that at the first order in θ_{so}, the temperature dependence has the form θ_{so}/kT where the spin Hall angle θ_{so} is proportional to the amplitude of the effective magnetic field. This is Curie's law that describes the paramagnetic behavior of the spin accumulation.

In order to summarize, we see that three main properties of the spin accumulation are derived in the limit $l_{sf} \gg \ell$: (a) The linearity with y, (b) the linearity with the applied voltage ΔV, and (c) the proportionality with $1/T$ for nondegenerate conductors. From a more quantitative viewpoint, the spin accumulation at the border is of the order of $n^{Sp}(y = \ell)/n_0 \approx \theta_{so}\, q \Delta V / kT$. The magnitude of the relative spin accumulation is expected to be of the order of 1% for a applied electric field of 5 mV/μm at 30 K with $\theta_{SH} \approx 10^{-4}$.

Furthermore, if both the device and its environment are **symmetric,** we have $C_E = 0$. The sum of the two Eqs. (18) at the first order in $\delta n_\updownarrow / n_0$ gives

$$\frac{\delta n^Q(y)}{n_0} = 0, \tag{21}$$

and the relation $\delta n_\uparrow = -\delta n_\downarrow$ is verified. Let us define the inhomogeneous part of the longitudinal current $\delta J_{x\updownarrow} = J_{x\updownarrow} - J_x^0$ produced by the spin-orbit field. According to the expression Eq. (15), $\delta J_{x\updownarrow}$ is a *pure spin current* in the sense that the inhomogeneous part of the current of electric charges δJ_x^Q is zero and the current of spins J_x^{Sp} is proportional to the spin accumulation $n^{Sp}(y)$,

$$\delta J_x^Q = \delta J_{x\uparrow} + \delta J_{x\downarrow} = 0 \quad \text{and}$$
$$J_x^{Sp} = \delta J_{x\uparrow} - \delta J_{x\downarrow} = J_x^0 \frac{n^{Sp}}{n_0}. \tag{22}$$

This stationary state corresponds to symmetric SHE devices as sketched in Fig. 1 and Fig. 2. Note that, according to Eq. (20), the spin current J_x^{Sp} [Eq. (22)] is proportional to the square of the injected current density $\pm(J_x^0)^2$. The Joule heating is thus expected to be a power four of the injected current, which is not without consequence for the heat produced inside the device [53].

However, if the device or its environment is **not symmetric** (typically if a supplementary layer is deposited on one side of the device), the typical length C_E defined in Eq. (18) is not zero and there is an asymmetry of the charge accumulation and spin polarization between the two edges. The following charge accumulation appears:

$$\frac{\delta n^Q(y)}{n_0} = \frac{C_E}{\lambda_D \sqrt{2}} \frac{sh\left(\frac{\sqrt{2}}{\lambda_D} y\right)}{ch\left(\frac{\sqrt{2}}{\lambda_D} \ell\right)}, \tag{23}$$

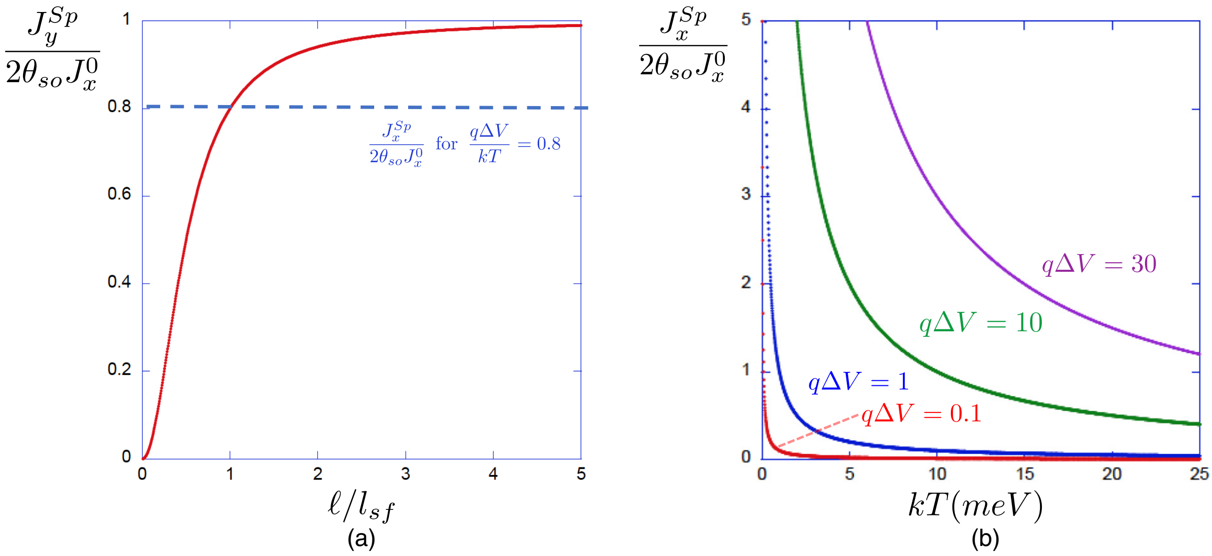

FIG. 3. (a) Transverse pure spin current J_y^{Sp} [Eq. (37) in the text] as a function the ratio $\ell/l_{\rm sf}$ of the width of the spin Hall bar over the spin-flip scattering length [Eq. (37) and Eq. (36)]. (b) Longitudinal pure spin current J_x^{Sp} as a function of the temperature [Eq. (39)] and [Eq. (20)] for different values of the injected voltage $q\Delta V$, expressed in *meV*. The amplitude is calculated for $y = L = \ell$. The currents are normalized by the product of the injected current $2J_x^0$ by the spin Hall angle $\theta_{\rm so}$ at the first order in $\theta_{\rm so}$.

and residual spin Hall voltage is generated. This result seems to be in agreement with the discussion developed in Ref. [54].

IV. APPROXIMATION OF LOCALIZED SPIN-FLIP SCATTERING AT THE EDGES ($l_{\rm sf} \ll \ell$)

The previous section describes the case of negligible spin-flip scattering, i.e., large spin-diffusion length with respect to the width of the spin Hall bar. In this section we will explore the *opposite limit*, for short spin-diffusion length with respect to the spin Hall bar $l_{\rm sf} \ll \ell$. This situation can be described by a spin-flip scattering that occurs locally at the edges. This approximation is usual in practice, since the spin Hall bar should be large enough for magneto-optic measurements.

Let us first define $\Delta\mu_0$ such that

$$\Delta\mu_0 \;=\; \int_{-\ell}^{+\ell} dy\, \partial_y \mu_\uparrow \;-\; \int_{-\ell}^{+\ell} dy\, \partial_y \mu_\downarrow. \tag{24}$$

The subscript 0 points out that the potential difference is evaluated between $y = +\ell$ and $y = -\ell$. Note that due to the translation invariance along x we have $\partial_x \Delta\mu = 0$ and $\partial_x \mu_\uparrow = \partial_x \mu_\downarrow$. In the framework of our approximation, the power dissipated by the spin-flip scattering is a constant given by $P_{\rm sf} = v\,\mathcal{L}\,\Delta\mu_0^2$, where $v = 2S_{\rm lat}\ell$ is the volume of the device. Inserting the transport equations (5) and (6) into Eq. (24) gives

$$\Delta\mu_0 \;=\; \frac{-\Delta A}{q\eta\left(1+\theta_{\rm so}^2\right)}, \tag{25}$$

where ΔA is given by the integrals

$$\Delta A = \int_{-\ell}^{+\ell} dy\, \frac{J_{y\uparrow} + \theta_{\rm so} J_{x\uparrow}}{n_\uparrow} - \int_{-\ell}^{+\ell} dy\, \frac{J_{y\downarrow} - \theta_{\rm so} J_{x\downarrow}}{n_\downarrow}. \tag{26}$$

The reduced dissipated power $\tilde{P} = \frac{q\eta(1+\theta_{\rm so}^2)}{S_{\rm lat}} P$ then reads

$$\begin{aligned}\tilde{P} \;&=\; \tilde{P}_J + \tilde{P}_{\rm sf}\\ &=\; \int_{-\ell}^{+\ell} \left(\frac{J_{x\uparrow}^2 + J_{y\uparrow}^2}{n_\uparrow} + \frac{J_{x\downarrow}^2 + J_{y\downarrow}^2}{n_\downarrow} \right) dy \;+ \alpha\,(\Delta A)^2\end{aligned} \tag{27}$$

expressed as a function of the control parameter α, defined by

$$\alpha = \frac{\mathcal{L}\,2\ell n_0}{\sigma_0\left(1+\theta_{\rm so}^2\right)} = \frac{n_0 \ell}{l_{\rm sf}^2\left(1+\theta_{\rm so}^2\right)}. \tag{28}$$

We used Eq. (8) for the expression of α as a function of the spin-flip scattering length $l_{\rm sf}$, which is well known in the context of the giant magnetoresistance effects. The functional of the dissipated power now reads

$$\begin{aligned}&\mathcal{F}[J_{x\updownarrow}, J_{y\updownarrow}, n_\updownarrow]\\ &= \int_{-\ell}^{\ell} \Bigg[\left(\frac{J_{x\uparrow}^2 + J_{y\uparrow}^2}{n_\uparrow} + \frac{J_{x\downarrow}^2 + J_{y\downarrow}^2}{n_\downarrow} \right)\\ &\qquad - \lambda_J\,(J_{x\uparrow} + J_{x\downarrow}) - \lambda_n\,(n_\uparrow + n_\downarrow) \Bigg] dy + \alpha(\Delta A)^2,\end{aligned} \tag{29}$$

and its minimization leads to the stationarity conditions. The functional derivation as a function of $J_{x\updownarrow}$ gives

$$\frac{\delta\mathcal{F}}{\delta J_{x\updownarrow}} = 0 \iff \pm 2\,\alpha\,\theta_{\rm so}\Delta A + 2J_{x\updownarrow} = n_\updownarrow \lambda_J. \tag{30}$$

The Lagrange coefficient λ_J is determined using the global conditions Eq. (9) and Eq. (10) on currents and charges for the sum of the two channels,

$$\lambda_J = \frac{2J_x^0}{n_0}. \tag{31}$$

Reinserting Eq. (31) into Eq. (30) gives the longitudinal currents as a function of the spin-dependent density of electric charges,

$$J_{x\updownarrow}(y) = \frac{n_\updownarrow(y)}{n_0} J_x^0 \mp \alpha\theta_{\rm so}\,\Delta A. \tag{32}$$

On the other hand, the minimization as a function of $J_{y\updownarrow}$ gives the current across the spin Hall bar,

$$\frac{\delta\mathcal{F}}{\delta J_{y\uparrow}} = 0 \iff J_{y\updownarrow} = \mp\alpha\,\Delta A. \tag{33}$$

Equation (33) shows that the transverse current $J_{y\updownarrow}$ is constant. Furthermore, $J_{y\updownarrow}$ is a *pure spin current*, in agreement with the results known from the direct resolution of the spin-dependent drift-diffusion equations [10,13–15,18]. Indeed, the charge current vanishes $J_y^Q \equiv J_{y\uparrow}^0 + J_{y\downarrow}^0 = 0$, and the spin current reads $J_y^{Sp} \equiv J_{y\uparrow}^0 - J_{y\downarrow}^0 = 2J_{y\uparrow}^0$.

Inserting the expression of the transverse current Eq. (33) into the expressions of the longitudinal current Eq. (32) divided by the density $n_\updownarrow$, the sum over the two channels then reads

$$\frac{J_{x\uparrow}}{n_\uparrow} + \frac{J_{x\downarrow}}{n_\downarrow} = \frac{2J_x^0}{n_0} + \theta_{so} J_y^0 \left(\frac{1}{n_\uparrow} - \frac{1}{n_\downarrow} \right). \tag{34}$$

In order to simplify as much as possible the physical interpretation, we continue the derivation at the first order in the accumulation $\delta n_\updownarrow / n_0$ (which is a realistic case). This approximation leads also to the first order in $\delta J_{x\updownarrow}/J_x^0$. Equation (26) then becomes $\Delta A \approx \frac{4\ell}{n_0}(J_y^0 + \theta_{so} J_x^0)$ so that the stationarity condition Eq. (33) reads

$$J_{y\updownarrow} = \mp \frac{\tilde{\alpha}}{1+\tilde{\alpha}} \theta_{so} J_x^0, \tag{35}$$

where we have introduced the *dimensionless parameter*

$$\tilde{\alpha} = \frac{4\ell\alpha}{n_0} = \frac{4\ell^2}{l_{sf}^2 \left(1 + \theta_{so}^2\right)}. \tag{36}$$

The curve J_y^{Sp} [Eq. (35) with Eq. (36)] is plotted in Fig. 3(a) as a function of the ratio ℓ/l_{sf}. We see that the current J_y^0 is composed of the same current as that expected in a Corbino disk of the same material [32,55], i.e., $J_{y\updownarrow}^{Corbino} = \mp \theta_{so} J_x^0$, but weighted by the coefficient $\tilde{\alpha}/(\tilde{\alpha}+1)$, where the control parameter $\tilde{\alpha}$ is given by Eq. (36).

(1) Note that in the case of small spin-flip scattering, i.e., $l_{sf}/\ell > 1$, the control parameter $\tilde{\alpha}$ goes to zero and $J_{y\updownarrow} \to 0$, which is indeed the result obtained in the approximation treated in the previous section.

(2) In the other limit of strong spin-flip scattering, i.e., small spin-diffusion length $l_{sf}/\ell \ll 1$, the ratio $\tilde{\alpha}/(1+\tilde{\alpha})$ is close to 1, and the spin currents $J_{y\updownarrow}$ are maximum, like in the Corbino disk. The presence of this transverse pure spin current with $\tilde{\alpha} = 1$ is the major feature of the SHE as described in previous theories (i.e., without taking into account the out-of-equilibrium electric screening).

The transverse charge and spin currents then read

$$J_y^Q(y) = 0 \quad \text{and} \quad J_y^{Sp}(y) = 2J_y^0 = -2\frac{\tilde{\alpha}}{1+\tilde{\alpha}} \theta_{so} J_x^0, \tag{37}$$

where $J_y^0 = J_{y\uparrow}^0 = -J_{y\downarrow}^0$.

The longitudinal spin currents Eq. (32) with Eq. (33) now read

$$J_{x\updownarrow}(y) = \left(\frac{n_\updownarrow(y)}{n_0} \mp \frac{\tilde{\alpha}}{1+\tilde{\alpha}} \theta_{so}^2 \right) J_x^0. \tag{38}$$

The solution Eq. (15) found for $J_{x\updownarrow}$ in the case without spin flip is now corrected by a small term proportional to θ_{so}^2. The longitudinal charge current and the longitudinal spin current are given by the expressions

$$J_x^Q(y) = J_x^0 \left(2 + \frac{\delta n^Q(y)}{n_0} \right) \quad \text{and}$$
$$J_x^{Sp}(y) = J_x^0 \left(\frac{n^{Sp}(y)}{n_0} - 2\frac{\tilde{\alpha}}{1+\tilde{\alpha}} \theta_{so}^2 \right). \tag{39}$$

In conclusion, the stationary state for the spin Hall bar for $l_{sf} \ll \ell$ and at the first order in $\delta n_\updownarrow / n$ is simply defined by Eq. (35) and Eq. (38), where the expression of $n_\updownarrow$ is given by the solution of the Poisson law Eq. (2). At the first order in θ_{so}, the stationary states obtained in the previous section are recovered; there is a solution of continuity between the two opposite approximations used in this study. The following paragraphs are devoted to the calculation of the densities $n_\updownarrow(y)$.

Injecting Eq. (35) and Eq. (38) into Eq. (6) in order to obtain $\partial_y \mu$, the Poisson law Eq. (2) reads now at the first order in $\delta n_\updownarrow / n_0$

$$\partial_y^2 (\delta n_\updownarrow) \mp \frac{\lambda_{SH}}{\lambda_D^2} \left(1 \pm \theta_{so}^2\right) \partial_y (\delta n_\updownarrow) - \frac{\delta n^Q}{\lambda_D^2} = 0, \tag{40}$$

where we have define the spin Hall characteristic length under spin-flip scattering as

$$\lambda_{SH} \equiv \frac{\epsilon}{q^2 \eta n_0^2} \frac{J_y^0}{1+\theta_{so}^2} = -\frac{\tilde{\alpha}}{1+\tilde{\alpha}} \lambda_{SH}^0, \tag{41}$$

where λ_{SH}^0 is the spin Hall length with negligible spin-flip scattering defined in Eq. (19). Since the measured spin-Hall angle verifies $\theta_{so} \ll 1$, Eq. (40) can be approximated at the first order in θ_{so}. Summing and subtracting the equations Eq. (40) for the two channels, we have the coupled equations

$$\frac{\partial_y^2 n^{Sp}}{n_0} - \frac{\lambda_{SH}}{\lambda_D^2} \frac{\partial_y \delta n^Q}{n_0} = 0, \tag{42}$$

$$\frac{\partial_y^2 \delta n^Q}{n_0} - \frac{\lambda_{SH}}{\lambda_D^2} \frac{\partial_y n^{Sp}}{n_0} - \frac{2}{\lambda_D^2} \frac{\delta n^Q}{n_0} = 0. \tag{43}$$

In the case of symmetrical device and electrical environment ($C_E = 0$), the spin accumulation is an odd function of y, and the solutions of Eq. (42) and Eq. (43) are

$$\frac{n^{Sp}(y)}{n_0} = a\, y + b\, \mathrm{sh}\left(\frac{y}{\lambda_m}\right) \tag{44}$$

and

$$\frac{\delta n^Q(y)}{n_0} = c + d\, \mathrm{ch}\left(\frac{y}{\lambda_m}\right), \tag{45}$$

where a, b, c, and d are the integration constants defined by the global constraints and symmetries (see the next section). The *typical spin Hall diffusion length* λ_m is given by the expression

$$\lambda_m = \frac{\lambda_D}{\sqrt{2 + \left(\frac{\tilde{\alpha}}{1+\tilde{\alpha}} \frac{\lambda_{SH}^0}{\lambda_D}\right)^2}}. \tag{46}$$

Note that the charge accumulation $\delta n^Q(y)$ is an even function of y. The voltage difference $\Delta V = 0$ is zero between the two edges of the device like in the case without spin flip (for $C_E = 0$).

V. DISCUSSION

From a more quantitative viewpoint, the expression Eq. (46) can be simplified due to the small value of the Debye-Fermi length λ_D. Indeed, the maximal value is of the order of some few microns, $\lambda_D^2 < 10^{-10}\ m^2$. On the other hand, the quantitative evaluation of the ratio $\lambda_{SH}^0/\lambda_D^2 \approx \theta_{so}\,(\frac{q\Delta V}{kT})\frac{1}{L}$, *typically smaller than the unity* (in m^{-1}), has been performed in the previous section below Eq. (20). This quantity depends on the intensity of the voltage ΔV imposed by the generator, but it is limited for experimental reasons (especially the limit of electromigration) and is also due to the limit of validity of our model (semiclassical diffusive process for which $n^{Sp}/n_0 < 1$). As a consequence, the product $(\lambda_{SH}^0/\lambda_D^2)^2\,\lambda_D^2$ is negligible with respect to 2 in Eq. (46). Since we have $\tilde{\alpha}/(1+\tilde{\alpha}) \leqslant 1$, we expect $\lambda_m \approx \lambda_D/\sqrt{2}$ whatever the value of the ratio l_{sf}/ℓ.

Furthermore, if we apply the global condition Eq. (9) $\int \delta n^Q(y)dy = 0$, we obtain a relation between a and b. A supplementary condition is necessary for the full determination of the coefficients a and b (see below). However, we have already a surprising result that should be pointed out about the stationary solution [Eq. (44)]. Indeed, the ratio of the hyperbolic term over the linear term in Eq. (44) is now univocally defined, and we have

$$\frac{b\,sh(y/\lambda_m)}{ay} \leqslant \frac{b\,sh(\ell/\lambda_m)}{a\ell} = \frac{1}{2}\left(\frac{\tilde{\alpha}}{1+\tilde{\alpha}}\right)^2\left(\frac{\lambda_{SH}^0}{\lambda_D}\right)^2. \quad (47)$$

According to the above discussion, $\lambda_{SH}^0/\lambda_D^2$ is upper bounded by one so that the ratio is below or of the order of λ_D^2 and *the contribution of the hyperbolic term seems to be negligible in usual conditions*. Equation (44) thus reduces to $\frac{n^{Sp}(y)}{n_0} \approx a\,y$. Furthermore, the parameter b is proportional to $(\frac{\tilde{\alpha}}{1+\tilde{\alpha}})^2$ that tends to zero for $l_{sf}/\ell \gg 1$: The stationary state under spin-flip converges to the stationary state defined without spin-flip calculates in Sec. III.

The condition of a continuity solution for all values of l_{sf} leads to the determination of the coefficients a and b,

$$a = -4\frac{\lambda_m^2}{\lambda_D^2}\left(\frac{\lambda_{SH}^0}{\lambda_D^2}\right) \approx -2\frac{\lambda_{SH}^0}{\lambda_D^2}, \quad (48)$$

and

$$b = -2\frac{\ell\lambda_m^2}{\mathrm{sh}\left(\frac{\ell}{\lambda_m}\right)}\left(\frac{\lambda_{SH}^0}{\lambda_D^2}\right)^3\left(\frac{\tilde{\alpha}}{1+\tilde{\alpha}}\right)^2. \quad (49)$$

The spin accumulation Eq. (44) is plotted in Fig. 4. On the other hand, the constant for the charge accumulation Eq. (45) is

$$c = -2\frac{\tilde{\alpha}}{1+\tilde{\alpha}}\,\lambda_m^2\left(\frac{\lambda_{SH}^0}{\lambda_D^2}\right)^2, \quad (50)$$

whose maximum value is of the order of $\lambda_D^2 a^2$, i.e., small, and

$$d = 2\frac{\lambda_m\ell}{\mathrm{sh}\left(\frac{\ell}{\lambda_m}\right)}\left(\frac{\lambda_{SH}^0}{\lambda_D^2}\right)^2\left(\frac{\tilde{\alpha}}{1+\tilde{\alpha}}\right), \quad (51)$$

so that the maximum value of the second term $d\mathrm{ch}(y/\lambda_m)$ in the right-hand side of Eq. (45) is of the order $\lambda_D a^2$. The linear part of the charge accumulation is negligible and the profile is hyperbolic, as for the case without spin-flip treated in Sec. III.

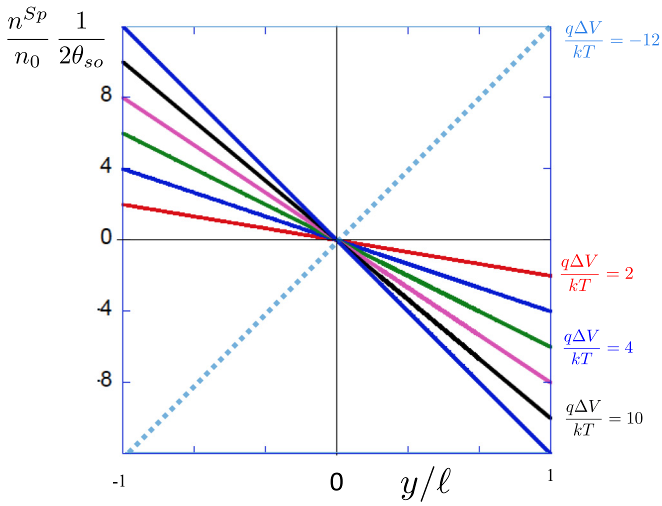

FIG. 4. Spin accumulation n^{Sp} [Eq. (20) in the text] as a function the ratio y/ℓ for different values of the ratio $q\Delta V/kT$, from $q\Delta V/kT = 2$ to $q\Delta V/kT = 12$. The spin accumulation is normalized by the product of the density of carriers at equilibrium $2n_0$ by the spin Hall angle θ_{so}. The curve for $q\Delta V/kT = -12$ shows that reversing the electric polarity reverses the sign of the spin accumulation.

Accordingly, it seems that the role of the spin-flip scattering is negligible for both spin accumulation and charge accumulation. In usual conditions, the unique qualitative effect of spin-flip scattering in the SHE is the generation of the transverse spin current J_y^{Sp}. The result of the linear dependence on y is confirmed by the observations performed by Bottegoni *et al.* [9] on devices for which the spin-diffusion length l_{sf} is large in absolute value but still smaller or of the same order than the width ℓ of the spin Hall bar. The measurements indeed show that the spin accumulation is linear in y, linear in ΔV, and inversely proportional to the temperature, in agreement with our results.

VI. CONCLUSION

The stationary state of the spin Hall bar has been studied in the framework of a variational approach that includes nonequilibrium screening effects. It is shown that the minimization of the heat power under the global constraints (global galvanostatic conditions and global electroneutrality) then allows the stationary state to be defined univocally. Indeed, the values of the current density and carrier density at the edges are imposed by the system itself in reaction to both the current injected by the generator and the static effective magnetic field. These values at the edges can thus hardly be used as fixed boundary conditions in order to solve the spin-dependent drift-diffusion equation.

Since the nonequilibrium screening effect modifies the current densities [generating a pure spin current $J_x^{Sp}(y) \neq 0$], it appears to be one of the main properties to be considered in order to define the stationary state. Note, however, that due to the small values of the Debye-Fermi length λ_D with respect to the other typical length scales, the amplitude of the spin accumulation $n^{Sp}(y)$ does not seem to depend crucially on λ_D.

The calculation is performed within the two limiting cases that are the negligible spin-flip scattering limit $l_{sf}/\ell \gg 1$ and the strong spin-flip scattering limit $l_{sf}/\ell \ll 1$ (where l_{sf} is the spin-flip scattering length and ℓ is the width of the spin Hall bar). In both cases, the profile of the spin accumulation $n^{Sp}(y)$ and the spin currents $\vec{J}_{\updownarrow}(y)$ can be described analytically. The two limits coincide, and simple expressions are given at the first order in the spin accumulation.

In the approximation of negligible spin-flip scattering, the main result is the absence of transverse currents $J_{y\updownarrow} = 0$ with a longitudinal spin current $J_x^{Sp}(y)$ proportional to the spin accumulation $n^{Sp}(y)$. The spin accumulation $n^{Sp}(y)$ is shown to be linear in y (across the device), linear in the electric field imposed by the generator along the x axis (i.e., linear to the injected current J_x^0), and inversely proportional to the temperature for nondegenerate conductors. The maximal order of magnitude expected for the spin accumulation is $n^{Sp}/n_0 \approx 1\%$ for $\theta_{SH} \approx 10^{-4}$ in an electric field of the order of $5\,\mathrm{mV}/\mu\mathrm{m}$ at $30\,K$.

In the case of strong spin-flip scattering, the main difference with the case of negligible spin-flip is the presence of a transverse pure spin current J_y^{Sp}, which flows across the sample, as predicted by the usual spin-dependent drift-diffusion model. However, this current is weighted by the factor $\tilde{\alpha}/(1+\tilde{\alpha})$ [Eq. (35)], where $\tilde{\alpha} \approx (2\ell/l_{sf})^2$ [Eq. (36)]. This multiplying factor describes the transition from a strong spin-flip scattering regime to a weak spin-flip scattering regime for which the transverse spin current vanishes.

Furthermore, it is shown that if the spin Hall bar is asymmetric, a voltage is generated between the two edges described by the parameter C_E [Eq. (23)]. This voltage should be present if a material is deposited on one side of the spin Hall bar. A more detailed description of a spin-dependent effect due to the deposition of a magnetic layer will be the object of forthcoming developments.

ACKNOWLEDGMENTS

We thank Felix Faisant for his important contribution to the initial development of this work, Miguel Rùbi for his support, Pierre-Michel Déjardin for the stochastic description, and Serge Boiziau for valuable discussions.

[1] Y. K. Kato, R. C. Myers, A. C. Gossard, and D. D. Awschalom, Observation of the spin Hall effect in semiconductors, Science **306**, 1910 (2004).
[2] N. P. Stern, R. C. Myers, V. R. Horowitz, A. C. Gossard, and D. D. Awschalom, Current-Induced Polarization and the Spin Hall Effect at Room Temperature, Phys. Rev. Lett. **97**, 126603 (2006).
[3] V. Sih, W. H. Lau, R. C. Myers, V. R. Horowitz, A. C. Gossard, and D. D. Awschalom, Generating Spin Currents in Semiconductors with the Spin Hall Effect, Phys. Rev. Lett. **97**, 096605 (2006).
[4] J. Wunderlich, B. Kaestner, J. Sinova, and T. Jungwirth, Experimental Observation of the Spin-Hall Effect in a Two-Dimensional Spin-Orbit Coupled Semiconductor System, Phys. Rev. Lett. **94**, 047204 (2005).
[5] S. O. Valenzuela and M. Tinkham, Direct electronic measurement of the spin-Hall effect, Nature (London) **442**, 176 (2006).
[6] T. Kimura, Y. Otani, T. Sato, S. Takahashi, and S. Maekawa, Room-Temperature Reversible Spin Hall Effect, Phys. Rev. Lett. **98**, 156601 (2007).
[7] S. Matsuzaka, Y. Ohno, and H. Ohno, Electron density dependence of the spin Hall effect in GaAs probed by scanning Kerr rotation microscopy, Phys. Rev. B **80**, 241305(R) (2009)
[8] C. Stamm, C. Murer, M. Berritta, J. Feng, M. Gaburac, P. M. Oppeneer, and P. Gambardella, Magneto-Optical Detection of the Spin Hall Effect in Pt and W Thin Films, Phys. Rev. Lett. **119**, 087203 (2017).
[9] F. Bottegoni, C. Zucchetti, S. Dal Conte, J. Frigerio, E. Carpene, C. Vergnaud, M. Jamet, G. Isella, F. Ciccacci, G. Cerullo, and M. Finazzi, Spin-Hall Voltage over a Large Length Scale in Bulk Germanium, Phys. Rev. Lett. **118**, 167402 (2017).
[10] M. I. Dyakonov and V. I. Perel, Possibility of orienting electron spins with current, Sov. Phys. JETP Lett. **13**, 467 (1971).
[11] M. I. Dyakonov, *Spin Physics in Semiconductors*, Springer Series in Solid-States Sciences (Springer Berlin, Heidelberg, 2008).
[12] J. E. Hirsch, Spin Hall Effect, Phys. Rev. Lett. **83**, 1834 (1999).
[13] Sh. Zhang, Spin Hall Effect in the Presence of Spin Diffusion, Phys. Rev. Lett. **85**, 393 (2000).
[14] W.-K. Tse, J. Fabian, I. Žutić, and S. Das Sarma, Spin accumulation in the extrinsic spin Hall effect, Phys. Rev. B **72**, 241303(R) (2005)
[15] S. Takahashi and S. Maekawa, Spin current, spin accumulation and spin Hall effect, Sci. Technol. Adv. Mater. **9**, 014105 (2008).
[16] A. Hoffmann, Spin Hall effects in metals, IEEE Trans. Magn. **49**, 5172 (2013).
[17] W. M. Saslow, Spin Hall effect and irreversible thermodynamics: Center-to-edge transverse current-induced voltage, Phys. Rev. B **91**, 014401 (2015).
[18] J. Sinova, S. O. Valenzuela, J. Wunderlich, C. H. Back, and T. Jungwirth, Spin Hall effects, Rev. Mod. Phys. **87**, 1213 (2015).
[19] J. Sinova and T. Jungwirth, Surprises from the spin-Hall effect, Phys. Today **70**(7), 38 (2017).
[20] M. J. Moelter, J. Evans, G. Elliott, and M. Jackson, Electric potential in the classical Hall effect: An unusual boundary-value problem, Am. J. Phys. **66**, 668 (1998);
[21] L. N. Trefenthen and R. J. Williams, Conformal mapping solution of Laplace's equation on a polygon with oblique derivative boundary conditions, J. Comput. Appl. Math. **14**, 227 (1986).
[22] D. R. Baker and J. P. Heremans, Linear geometrical magnetoresistance effect: Influence of geometry and material composition, Phys. Rev. B **59**, 13927 (1999).
[23] G. Zhang, J. Zhang, Z. Liu, P. Wu, H. Wu, H. Qian, Y. Wang, Z. Zhang, and Z. Yu, Geometry Optimization of Planar Hall Devices Under Voltage Biasing, IEEE Trans. Electron Devices **61**, 4216 (2014).
[24] O. Paul and M. Cornil, Explicit connection between sample geometry and Hall response, Appl. Phys. Lett. **95**, 232112 (2009).
[25] T. Kramer, V. Krueckl, E. J. Heller, and R. E. Parrott, Self-consistent calculation of electric potentials in Hall devices, Phys. Rev. B **81**, 205306 (2010).

[26] C. Fernandes, H. E. Ruda, and A. Shik, Hall effect in nanowires, J. Appl. Phys. **115**, 234304 (2014).
[27] D. Homentcovschi and R. Bercia, Analytical solution for the electric field in Hall plates, Z. Angew. Math. Phys. **69**, 97 (2018).
[28] S. A. Solin, T. Thio, D. R. Hines, and J. J. Heremans, Enhanced room-temperature geometric magnetoresistance in inhomogeneous narrow-gap semiconductors, Science **289**, 1530 (2000).
[29] L. M. Pugsley, L. R. Ram-Mohan, and S. A. Solin, Extraordinary magnetoresistance in two and three dimensions: Geometrical optimization, J. Appl. Phys. **113**, 064505 (2013).
[30] J.-E. Wegrowe, R. V. Benda, and J. M. Rubì, Conditions for the generation of spin current in spin-Hall devices, Europhys. Lett. **118**, 67005 (2017).
[31] J.-E. Wegrowe and P.-M. Dejardin, Variational approach to the stationary spin-Hall effect, Europhys. Lett. **124**, 17003 (2018).
[32] R. Benda, E. Olive, M. J. Rubì, and J.-E. Wegrowe, Towards Joule heating optimization in Hall devices, Phys. Rev. B **98**, 085417 (2018).
[33] M. Creff, F. Faisant, M. Rubì, and J.-E. Wegrowe, Surface current in Hall devices, J. Appl. Phys. **128**, 054501 (2020).
[34] P.-M. Déjardin and J.-E. Wegrowe, Stochastic description of the stationary Hall effect, J. Appl. Phys. **128**, 184504 (2020)
[35] F. Faisant, M. Creff, and J.-E. Wegrowe, The physical properties of the Hall current, J. Appl. Phys. **129**, 144501 (2021).
[36] L. Onsager and S. Machlup, Fluctuations and irreversible processes, Phys. Rev. **91**, 1505 (1953).
[37] S. Bruers, Ch. Maes, and K. Netocný, On the validity of entropy production principles for linear electrical circuits, J. Stat. Phys. **129**, 725 (2007).
[38] L. Bertini, A. De Sole, D. Gabrielli, G. Jona-Lasinio, and C. Landim, Minimum dissipation principle in stationary non-equilibrium sates, J. Stat. Phys. **116**, 831 (2004).
[39] E. H. Hall, On a new action of the magnet on electric currents, Am. J. Math. **2**, 287 (1879).
[40] M. Johnson and R. H. Silsbee, Interfacial Charge-Spin Coupling: Injection and Detection of Spin Magnetization in Metals, Phys. Rev. Lett. **55**, 1790 (1985).
[41] P. C. van Son, H. van Kempen, and P. Wyder, Boundary Resistance of the Ferromagnetic-Nonferromagnetic Metal Interface, Phys. Rev. Lett. **58**, 2271 (1987).
[42] T. Valet and A. Fert, Theory of the perpendicular magnetoresistance in magnetic mutilayers, Phys. Rev. B **48**, 7099 (1993).
[43] P. M. Levy and S. Zhang, Our current understanding of giant magnetoresisitance in transition-metal multilayers, J. Magn. Magn. Mater. **151**, 315 (1995).
[44] J.-E. Wegrowe, Thermokinetic approach of the generalized Landau-Lifshitz-Gilbert equation with spin-polarized current, Phys. Rev. B **62**, 1067 (2000).
[45] F. J. Jedema, M. S. Nijboer, A. T. Filip, and B. J. van Wees, Spin injection and spin accumulation in all-metal mesoscopic spin-valves, Phys. Rev. B **67**, 085319 (2003).
[46] G. Schmidt, D. Ferrand, L. W. Molenkamp, A. T. Filip, and B. J. van Wees, Fundamental obstacle for electrical spin injection from a ferromagnetic metal into a diffusive semiconductor, Phys. Rev. B **62**, R4790 (2000).
[47] D. L. Smith and R. N. Silver, Electrical spin injection into semiconductors, Phys. Rev. B **64**, 045323 (2001).
[48] A. Fert and H. Jaffrès, Condition for efficient spin injection from a ferromagnetic metal into a semiconductor, Phys. Rev. B **64**, 184420 (2001).
[49] J.-E. Wegrowe, Twofold stationary states in the classical spin-Hall effect, J. Phys.: Condens. Matter **29**, 485801 (2017).
[50] In the case of degenerate semiconductors and metals, the expression is valid at the first order in $\delta n/n_0$.
[51] D. Reguera, J. M. G. Vilar, and J. M. Rubì, The mesoscopic dynamics of thermodynamic systems, J. Phys. Chem. B **109**, 21502 (2005).
[52] L. Onsager, Reciprocal relations in irreversible processes II, Phys. Rev. **38**, 2265 (1931)
[53] A. Churikova, D. Bono, B. Neltner, A. Wittmann, L. Scipioni, A. Shepard, T. Newhouse-Illige, J. Greer, and G. S. D. Beach, Non-magnetic origin of spin Hall magnetoresistance-like signals in Pt films and epitaxial NiO/Pt bilayers, Appl. Phys. Lett. **116**, 022410 (2020).
[54] Y. V. Pershin and M. Di Ventra, A voltage probe of the spin Hall effect, J. Phys.: Condens. Matter **20**, 025204 (2008).
[55] B. Madon, M. Hehn, F. Montaigne, D. Lacour, and J.-E. Wegrowe, Corbino magnetoresistance in ferromagnetic layers: Two representative examples $Ni_{81}Fe_{19}$ and $Co_{83}Gd_{17}$, Phys. Rev. B **98**, 220405(R) (2018).